Choosing an Appropriate Spatial Resolution for Remote Sensing Investigations

Peter M. Atkinson and Paul J. Curran

Abstract

Choosing rationally the spatial resolution for remote sensing requires a formal relation between the size of support and some measure of the information content. The local variance in the image has been used to help choose an appropriate spatial resolution. Here we choose spatial resolutions to map continuous variation in properties, such as biomass, using the variogram. The experimental variogram can be separated into components of underlying spatially dependent variation and measurement error. The spatially dependent component can be deregularized to a punctual support, and then regularized to any spatial resolution. The regularized variogram summarizes the information attainable by imaging at that spatial resolution because information exists in the relations between observations only. The investigator can use it to select a combination of spatial resolution and method of analysis for a given investigation. Two examples demonstrate the method.

Introduction

If the Earth were spatially uniform, then the signal of a given area of ground would be the same as that from its neighbor and there would be no relation between spatial resolution and signal strength. In practice, however, the Earth is spatially variable and the frequency of this variability determines the form of this relation between spatial resolution and signal strength (Raffy, 1993; Raffy, 1994). To characterize this important relation, we need to use the techniques of geostatistics. Throughout this paper, the geostatistical concept of the support (the size, geometry, and orientation of the space over which measurement is made) is taken to be equivalent to spatial resolution. In practice, the geometry of the support is complex, and the true size of support is much greater than the spatial resolution because of the point spread function (PSF) of the sensor. Further, the true support varies across the image as a result of, for example, the terrain and the scan angle of the sensor.

The spatial resolutions of current sensors vary over four or five orders of magnitude, so investigators have a wide choice. But on what criteria should an investigator choose a spatial resolution? Ideally, the spatial resolution should be chosen so that the information desired is attained with the least data. The question then is, How should the investigator decide when the desired information has been attained, and with the least data? Usually, the choice is intuitive, and in some cases the investigator uses what happens to be readily available. As a result, the spatial resolution may be inappropriate, so that the information desired may not be obtained, or unnecessary data may be acquired (Lam and Quottrochi, 1992; McGwire et al., 1993).

In remote sensing, most studies on spatial resolution have examined the accuracy of estimating some property at the ground with remotely sensed imagery of different spatial resolutions. For example, Latty and Hoffer (1981), Welch (1982), Bizzell and Prior (1983), Toll (1983), and Johnson and Howarth (1987) examined the effect of spatial resolution on the accuracy of remotely sensed classifications of land cover. These studies are empirical, and the choice of spatial resolution depends on the relation between two variables. To develop a theoretical approach, we initially limit ourselves to the relations among observations of one property only.

Researchers in agronomy were the first to show interest in the size of support. Mercer and Hall (1911) measured the yields of crops in small plots in uniformity trials. Then, by grouping the plots into ever larger ones, they discovered that the plot-to-plot variance decreased only slightly for sizes greater than about 0.01 ha, and this became the recommended size of plot in field experiments for many years. Smith (1938), working in Australia, found an empirical linear relation between the log of dispersion (or sample) variance and log of size of support.

Mercer and Hall (1911) and Smith (1938) demonstrated that the variance between sample values decreases as the support increases in size. The precision of estimating the *mean* of some property within a region increases with size of support because the variance decreases. In the context of remote sensing, Curran and Williamson (1988) demonstrated this relation for estimating the mean green leaf area index (GLAI) of a region.

If the objective is to *map* some property, then the variation between sample observations determines both the precision of the estimates and the *information* that is ultimately displayed (Dungan et al., 1994). Both precision and information are valid criteria on which to base a choice of spatial resolution (Atkinson and Curran, 1995). However, if the spatial sample is the map (for example, if complete coverage is provided and there is no interpolation to be performed), then the spatial variation determines only the information that is displayed. Here, we consider the relation of information with spatial resolution and how it affects a choice of spatial resolution for mapping by remote sensing.

Woodcock and Strahler (1987) based a choice of spatial resolution on the relation between spatial resolution and spatial dependence, the likelihood that observations close in space are more alike than those further apart. The ideas are similar to those of Grieg-Smith (1964) and Moellering and Tobler (1972); they were extended in Jupp et al. (1988; 1989); and they were applied in a remote sensing context by Townshend and Justice (1988), Townshend et al. (1988), Chavez (1992), Gu (1992), and Vogt (1992). Woodcock and

Department of Geography, University of Southampton, Highfield, Southampton SO17 1BJ, United Kingdom (pma@soton.ac.uk).

Strahler (1987) represented spatial dependence with the local variance, defined as follows:

Let $z(x_{ij})$ be the value of the pixel located at x_{ij} in the ith row and jth column of an image. Then the local variance, σ_{ij}^2, around x_{ij} can be computed over a $(2n+1)$ by $(2m+1)$ window: i.e.,

$$\sigma_{ij}^2 = 1/[(2n + 1)(2m + 1)-1] \qquad (1)$$
$$\sum_{k=i-n}^{i+n} \sum_{l=j-m}^{j+m} \{z(x_{kl}) - \mu_{ij}\}^2$$

where u_{ij} is the mean of the $(2n+1)$ by $(2m+1)$ window centered on x_{ij}. If $m = n = 1$, then the local variance is computed over x_{ij} and its neighbors. The mean local variance for an image is taken to be the mean σ_{ij}^2 computed for all x_{ij} with the exception of a border equal to either n or m.

The mean local variance can be computed for different spatial resolutions, and it is as a function of spatial resolution that it represents the spatial dependence in the image. To measure the local variance at multiple spatial resolutions, the image is degraded to successively coarser spatial resolutions simply by combining pixels into larger ones and computing the average values in them.

The rationale behind Woodcock and Strahler's (1987) use of local variance is as follows. Scenes are assumed to be composed of discrete objects arranged either in a mosaic that completely covers the region, or distributed on a continuous background (Strahler et al., 1986). If the spatial resolution is much finer than the size of objects in the scene, many adjacent pixels will be alike and the local variance will be small. As the spatial resolution coarsens towards the size of the objects, the local variance will increase to a maximum. When the spatial resolution is much coarser than the size of the objects, the local variance will once again be small because local variation will be encompassed within the pixels.

The maximum in the local variance as a function of spatial resolution is an indirect guide to the size of objects in the scene. As such, it can be used to choose an appropriate combination of spatial resolution and method of analysis for specific investigations. For example, if one wishes to classify an image using a spectral classifier, one might select a spatial resolution that is much finer than the size of objects in the scene. Alternatively, if the spatial resolution chosen is similar to the size of objects in the scene, then a mixture model may be more appropriate.

For mapping continuous variation by remote sensing, the spatial resolution of the imagery should be fine enough to capture the variation of interest in the property at the ground and should, therefore, according to Woodcock and Strahler (1987), be much finer than the spatial resolution at which the local variance in the property at the ground occurs. If it is not, the spatial variation of interest in the property at the ground may be encompassed within the support.

Method

Woodcock and Strahler's (1987) method is attractive. However, we should recognize that it is strictly empirical, analogous to Mercer and Hall's (1911) approach above. It depends on coarsening the spatial resolution of imagery by computing average values. We suggest that the method can be improved by modeling images as realizations of random processes.

Model of Spatial Variation
Radiation sensed remotely may be represented by the following model:

$$Z(\mathbf{x}) = m_v + e(\mathbf{x}) \qquad (2)$$

where $Z(\mathbf{x})$ is a random function (RF) defined for positions $\mathbf{x}$

in two-dimensional space, $\mathbb{R}^2$; m_v is the local mean of Z in a local region V, a part of $\mathbb{R}^2$; and $e(\mathbf{x})$ is an RF with mean of zero.

Generally, the spatial variation in Z from place to place is such that we may adopt the so-called intrinsic hypothesis of stationarity (Matheron, 1965; Matheron, 1971) in which the mathematical expectation exists and does not depend on $\mathbf{x}$: i.e.,

$$\mathrm{E}\{Z(\mathbf{x})\} = m_v \qquad \text{for all } \mathbf{x}, \qquad (3)$$

and for all vectors of separation or lags, $\mathbf{h}$, the increment, $[Z(\mathbf{x}) - Z(\mathbf{x}+\mathbf{h})]$, has a finite variance which does not depend on $\mathbf{x}$: i.e.,

$$2\gamma(\mathbf{h}) = \mathrm{var}[Z(\mathbf{x}) - Z(\mathbf{x} + \mathbf{h})]$$
$$= \mathrm{E}\{[Z(\mathbf{x}) - Z(\mathbf{x} + \mathbf{h})]^2\} - (\mathrm{E}[Z(\mathbf{x}) - Z(\mathbf{x} + \mathbf{h})])^2 \qquad (4)$$
$$= \mathrm{E}\{[Z(x) - Z(\mathbf{x} + \mathbf{h})]^2\}$$

Here, $\gamma(\mathbf{h})$ is the variogram, a function which relates semivariance to lag $\mathbf{h}$, and which summarizes the spatial dependence in Z.

The variogram as defined above is for a punctual support, whereas in practice our measurements are made on pixels of a finite area. If we denote an observation or pixel v with area $|v|$, then we are concerned with the spatial means, $Z_v(\mathbf{x})$, which are the integrals of $Z(\mathbf{x})$ over v: i.e.,

$$Z_v(\mathbf{x}) = \frac{1}{|v|} \int \int_{v(x)} Z(y)\,dy \qquad (5)$$

where $Z(\mathbf{y})$ is the variable Z defined on a punctual support.

The variogram, $\gamma_v(\mathbf{h})$, on some support v is readily obtained from the punctual variogram by (Journel and Huijbregts, 1978)

$$\gamma_v(\mathbf{h}) = \bar{\gamma}(v, v_{\mathbf{h}}) - \bar{\gamma}(v,v) \qquad (6)$$

Here, $\bar{\gamma}(v,v_{\mathbf{h}})$ is the average punctual semivariance between two pixels of area $|v|$ whose centroids are separated by $\mathbf{h}$, and $\bar{\gamma}(v,v)$ is the average punctual semivariance within a pixel of area $|v|$.

The spatial integration is usually known as regularization (Clark, 1977; Jupp et al., 1988; Jupp et al., 1989; Isaaks and Srivastava, 1989; Zhang et al., 1992). Geometrically, regularization is simply increasing the size of support over which a spatial process is averaged. In the context of remote sensing, it means increasing the size of the pixels and coarsening the spatial resolution. Regularization is the key to understanding the relations among spatial dependence and size of support.

The Experimental Variogram and Measurement Error
We never know a priori the punctual variogram. Indeed, we rarely know the variogram on the support of the sensor, and this has to be found experimentally from data. The experimental variogram has been computed and applied extensively in the present context (Curran, 1988; Webster et al., 1989; Clark, 1990; Chavez, 1992; Rossi et al., 1992; Gohin and Langlois, 1993).

Provided we have measured some property, Z, on observations centered at $\mathbf{x}_1, \mathbf{x}_2, ...,$ we can compute an experimental variogram for $p(\mathbf{h})$ pairs of observations: i.e.,

$$\hat{\gamma}_v(\mathbf{h}) = 1/2p(\mathbf{h}) \sum_{l=1}^{p(\mathbf{h})} \{z(\mathbf{x}_l) - z(\mathbf{x}_l + \mathbf{h})\}^2 \qquad (7)$$

By changing $\mathbf{h}$, an ordered set of semivariances is obtained, and this constitutes the experimental variogram.

The experimental variogram, like the experimental variable from which it is computed, is likely to contain measure-

ment error. Because measurement implies integration over a support of positive size, the underlying variable is regularized and its variogram is continuous through the origin. The variogram of measurement error, however, does not pass through the origin. The experimental semivariance at a lag of zero, $\hat{\gamma}_v(0^+)$, is, therefore, expected to be some positive value determined solely by the measurement error in the variable (Curran and Dungan, 1989; Atkinson, 1993).

The quantities $\hat{\gamma}_v(\mathbf{h})$ estimate the semivariances on the experimental support, and, to proceed further, we must fit a mathematical model to them. This model must be "authorized" in that it cannot produce negative variances; technically, it must be conditionally negative semi definite (CNSD). There are several well established simple CNSD models, listed by Webster and Oliver (1990).

Variogram models often feature a term c_0, the nugget variance. This quantity is the intercept of the fitted model on the ordinate. While the nugget variance does not generally seek to estimate $\hat{\gamma}_v(0^+)$ it may be used for this purpose where observations are adjacent (or approximately so) as for remotely sensed imagery (Curran and Dungan, 1989).

Practical Regularization

In many fields such as mining and soil survey, the observations, $z(\mathbf{x}_l)$, $l=1, 2, ...$, for Equation 7 are so small in relation to the supports for which we want statistics that they can be approximated as being points and the experimental variogram may be regularized directly (Webster, 1991). Figure 1a shows an example in which a spherical model (given by Equation 8) is regularized over square supports of side 1 m: i.e.,

$$\gamma(h) = c_1 \{1.5\,(h/a_1) - 0.5\,(h/a_1)^3\} \text{ for all } 0 < h < a_1$$

$$\gamma(h) = c_0 + c_1 \qquad\qquad \text{for all } h > a_1 \qquad (8)$$

$$\gamma(0) = 0$$

where $h = |\mathbf{h}|$ for isotropic variation. The quantity c_1 is the structured variance of the model and is 10 units and a_1 is the range and is 10 m.

For remotely sensed imagery, the size of support is the maximum possible given the sampling intensity of the image, and may often be of the same order of magnitude as that to which we want to regularize. In these circumstances, we must first deregularize to estimate the punctual variogram.

In our surveys, the variables were measured on contiguous supports and there was no intervening space unaccounted for. The nugget variances are, therefore, likely to estimate measurement error accurately (Curran and Dungan, 1989). The relation of measurement error with size of support cannot be represented analytically, and so measurement error must be removed from the variograms and treated separately. The first step in deregularizing a variogram is to subtract the nugget variance, if it has one, leaving functions that pass through the origins.

For the present purpose, measurement error is of no interest and so it plays no further part in the analysis. When computing the local variance from digital images, measurement error is an integral part of the pixel values and is averaged at each new coarser spatial resolution. This is undesirable and may lead to bias in the spatial resolution at which the local variance is maximized. In particular, the local variance at the smallest lags will be smaller with the measurement error removed. This is one reason why we recommend that the measured spatial variation be modeled.

We must now try to find a model for the punctual variogram, which when regularized will produce a curve which matches the fitted function. We chose for each punctual vario-
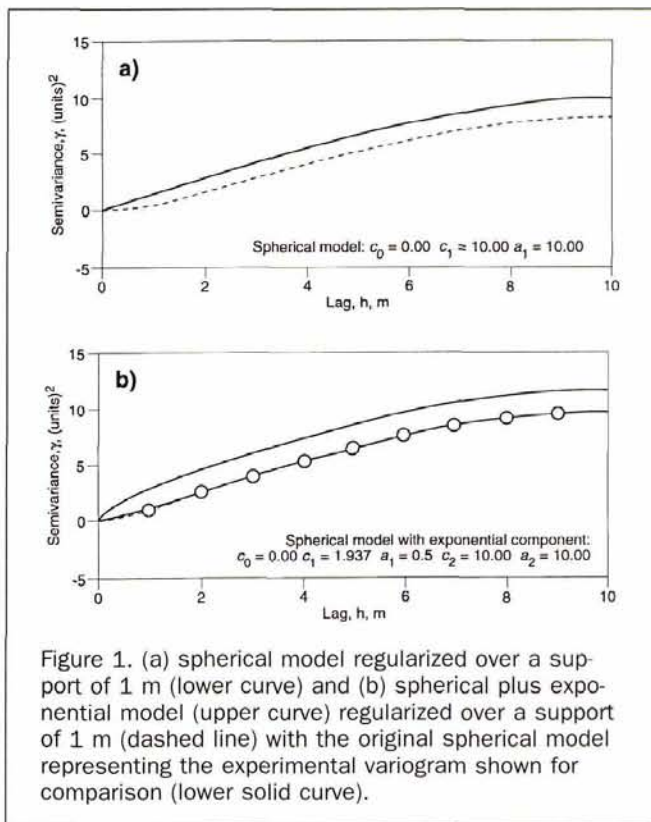

Figure 1. (a) spherical model regularized over a support of 1 m (lower curve) and (b) spherical plus exponential model (upper curve) regularized over a support of 1 m (dashed line) with the original spherical model representing the experimental variogram shown for comparison (lower solid curve).

gram the same basic function as that fitted to the experimental variogram. We added to this an exponential term, $c_e\{1 - \exp(-h/a_e)\}$, where $a_e=0.5d$, to represent the short-range variation within the experimental pixel of side d. Then, by iterative regularization, we adjusted c_e, the sill of the short-range term, until the sill of the regularized variogram equalled that of the fitted model within an acceptable tolerance. The final model of the punctual variogram is as follows:

$$\gamma(h) = c_e\{1 - \exp(-h/a_e)\} + c_1\{1.5\,h/a_1 - 0.5\,(h/a_1)^3\}$$

$$\text{for all } 0 < h < a_1 \qquad (9)$$

$$\gamma(h) = c_1 \quad \text{for all } h > a_1$$

$$\gamma(0) = 0$$

where c_e is 1.937 units, c_1 is 10 units, a_e is 0.5 m, and a_1 is 10 m. Figure 1b shows it, together with the variogram regularized over the experimental support (dashed line) and, for comparison, the fitted model (solid line) that it matches.

The variograms deregularized in this way are, thus, the basic functions from which to construct variograms that are of the same order of magnitude as the experimental ones.

Regularizing Variograms of Real Imagery

Experimental variograms were computed for real digital images degraded to successively coarser spatial resolutions. The algorithm used to degrade the imagery is the same as that used by Woodcock and Strahler (1987), simply averaging the pixel values that are encompassed within a single larger pixel. This involves the assumption of a square wave response which may be a crude approximation only of reality (Justice et al., 1989), but it will serve to demonstrate the method.

Two images recorded in the red wavelengths, both in England, were used. The first was a Daedelus AADS 1268 airborne multispectral scanner system (MSS) image of reclaimed grassland near Belper, Derbyshire and the second was a SPOT
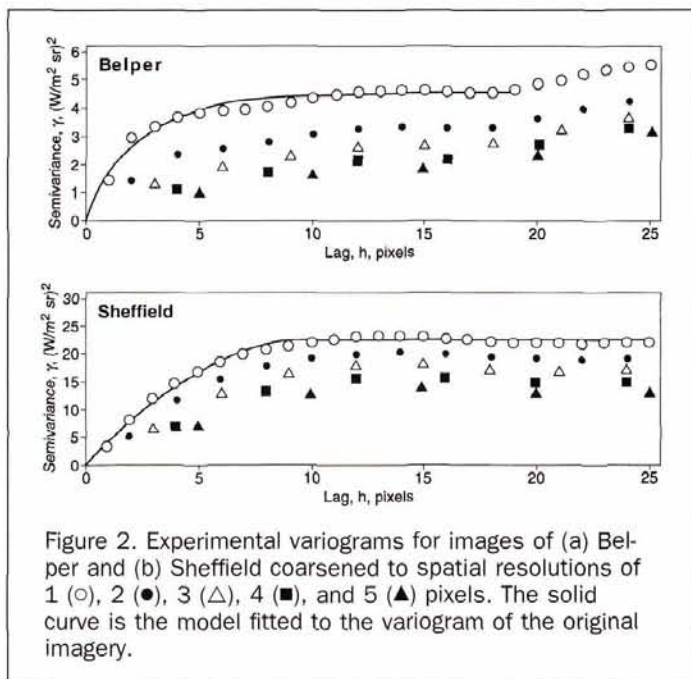
Figure 2. Experimental variograms for images of (a) Belper and (b) Sheffield coarsened to spatial resolutions of 1 (○), 2 (●), 3 (△), 4 (■), and 5 (▲) pixels. The solid curve is the model fitted to the variogram of the original imagery.

HRV image of urban Sheffield. The two images are very different. For example, the airborne MSS image of Belper has a spatial resolution of 1.5 m and the area of interest within the image is a field of pasture of some 300 m by 300 m. In contrast, the SPOT image has a spatial resolution of 20 m and the area of interest within the image is the city of Sheffield. The experimental variograms of the two initial and degraded images are shown in Figure 2.

The experimental variograms were modeled with the exponential (Belper) and penta-spherical (Sheffield) models (Table 1) (solid curves in Figure 2). The regularized variograms can be estimated from the models by deregularization and regularization using Equation 6. In order that the estimates correspond to the experimental variograms computed above by degrading the images, regularized variograms were obtained for square, non-overlapping supports (Figure 3). Allowing for the uncertainty in fitting a model to the experimental and regularized values of semivariance, there is correspondence between the empirically and analytically derived functions.

Identifying Scales of Variation
The local variance may be computed from the punctual variogram using Krige's relation (Journel and Huijbregts, 1978): i.e.,

$$D^2 (v/V) = \bar{\gamma} (V, V) - \tilde{\gamma} (v, v) \qquad (10)$$

where $D^2(v/V)$ is the dispersion variance of a sample defined on a support v within a region V.

The local variance is computed over a range of separating distances of between 0 pixels and $\sqrt{8}$ pixels (if $m = n = 1$). In terms of Krige's relation and the punctual semivariance, the local variance is computed over distances from 0 pixels up to the diagonal of a 3- by 3-pixel cell, that is, $\sqrt{18}$. This choice is somewhat arbitrary. Here, we replace the local variance with the semivariance at a lag of one support, $\hat{\gamma}_v(v)$ (Atkinson and Danson, 1988). Our reasons for doing so relate to the need to base a choice of spatial resolution on spatial information.

Information exists in the relations *between* measurements, represented by spatial dependence, and summarized by the variogram (Equation 6): information is relative. Further, information exists between immediate neighbors (Von Neuman, 1941). Relations between more distant observations are ac-

counted for by the intervening neighbors and represent double counting.

In $\mathbb{R}^1$, there are at most two neighbors of $z_v(\mathbf{x}_0)$, and all the information associated with $z_v(\mathbf{x}_0)$ exists in the two relations with them. In $\mathbb{R}^2$, $z_v(\mathbf{x}_0)$ can have many neighbors and so, to avoid double counting, each relation with each neighbor may be weighted according to the proportion of the Dirichlet tile associated with $z_v(\mathbf{x}_0)$ that is attributable to it (Atkinson, 1995). For remotely sensed imagery, the neighbors of a pixel, $z_v(\mathbf{x}_0)$, defined in terms of its Dirichlet tile, are the two horizontally adjacent and two vertically adjacent pixels, equally weighted. The information associated with a pixel v in an image may, therefore, be computed from the semivariance at a lag of one pixel $\hat{\gamma}_v(v)$.

Given an estimate of the punctual variogram, $\hat{\gamma}_v(v)$ may be computed for any size of support from Equation 6, including supports that are smaller than the experimental support. Further, $\hat{\gamma}_v(v)$ may be computed from small subareas of images, for example, within agricultural fields and from data that do not constitute an image, for example, from transect data. This is a direct advantage of modeling the spatial variation.

Clearly, $\hat{\gamma}_v(v)$ and the local variance are closely related. Figures 4a through 4d relate $\hat{\gamma}_v(v)$, the local variance, and the dispersion variance to size of support for a series of black shapes (square, circle, diamond, and cross) on a white background. The quantity $\hat{\gamma}_v(v)_{max}$ occurs at a slightly coarser spatial resolution than the maximum of the local variance as might be expected from Equations 6 and 10.

The graphs of the experimental $\hat{\gamma}_v(v)$ against spatial resolution are plotted for the images of Belper and Sheffield in Figures 5a, 5b, and 5c. One can see a relation between the shape of the initial experimental variogram model and the position of $\hat{\gamma}_v(v)_{max}$ on the abscissa. For both variograms, the model increases sharply from the origin. As a result, $\hat{\gamma}_v(v)_{max}$ is reached when the spatial resolution is about 2 pixels (3 m) and 5 pixels (100 m), respectively. For mapping, the spatial resolution should be much finer than these values.

Remote Sensing Examples
The following examples illustrate the procedure for selecting an appropriate size of support for mapping continuous variation by remote sensing.

Field Measurements
The study site was Morrell Wood opencast coal reclamation site, located 3 km east of Belper in Derbyshire, United Kingdom (UK). It lies at about 100 m in altitude with slopes varying between 0° and 8°. The site consists of grass fields separated by quickthorn hedging. The grassland was fairly uniform and dominated by *Lolium perenne* and *Lolium multiflorum* with some clover, *Trifolium repens*. Cattle and sheep grazed the pasture from time to time throughout the year.

On 6 May 1988, one measurement of reflectance was made using a Milton multiband radiometer (MMR) (Milton, 1980) over the center of each of 100 1- by 1-m plots along a 200-m transect. Simultaneous measurements were made over a Halon panel for conversion to reflectance. The reflectance properties of the Halon panel had been measured using an Infrared Intelligent Spectroradiometer (Milton and Rollin, 1987) and calibrated against the UK national standard. The NDVI was computed as follows:

TABLE 1. MODELS FITTED TO EXPERIMENTAL VARIOGRAMS OF IMAGERY OF BELPER AND SHEFFIELD

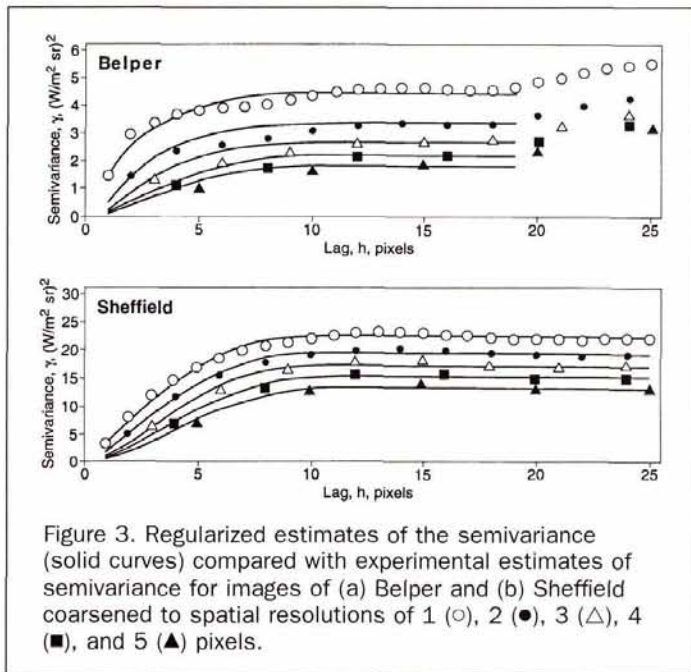| Image	Model	c_0	c_1	a_1
Belper	Exponential	—	4.554	2.425
Sheffield	Penta-spherical	—	22.71	11.08

Figure 3. Regularized estimates of the semivariance (solid curves) compared with experimental estimates of semivariance for images of (a) Belper and (b) Sheffield coarsened to spatial resolutions of 1 (○), 2 (●), 3 (△), 4 (■), and 5 (▲) pixels.
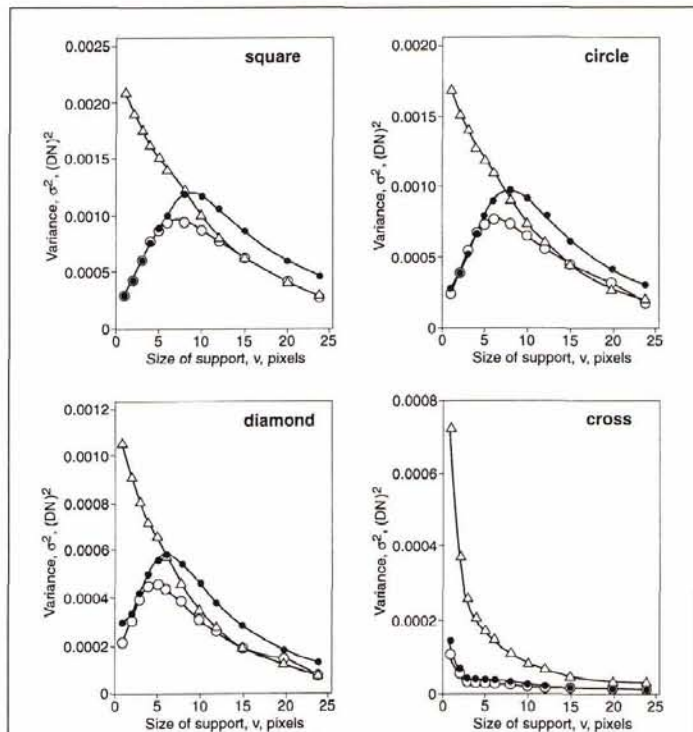

Figure 4. Local variance (○), the semivariance at a lag of one pixel (●), and the dispersion variance (△) plotted against size of support for four black shapes on a white background.

$$\text{NDVI} = (\text{NIR} - \text{Red})/(\text{NIR} + \text{Red}) \qquad (11)$$

where NIR is the reflectance in near-infrared wavelengths and Red is the reflectance in red wavelengths.

The above-ground biomass was weighed. A sample of approximately 80 g was weighed and dried for 24 hours at 65°C and reweighed to determine the dry biomass.

Estimating the Dry Biomass

The aim is to map the dry biomass at Belper on 6 May 1988 in a remote sensing investigation. We have chosen two hypothetical investigations. In the first, the aim is to map the dry biomass using ground-based radiometry and cokriging and, in the second, the aim is to map the dry biomass using airborne MSS imagery and regression.

Suppose that an investigator wishes to map the dry biomass by cokriging from samples of dry biomass and NDVI measured with a field radiometer (Atkinson et al., 1992). The variograms of dry biomass and NDVI must be computed for cokriging. Therefore, the investigator can use them for two valuable reconnaissance studies at no extra cost in the field. These are, first, designing an optimal sampling strategy (Atkinson et al., 1992) and second, choosing a suitable spatial resolution which we now consider. The choice of spatial resolution should depend on the property at the ground, not the remotely sensed imagery. Therefore, we start with the dry biomass measured along a 200-m transect.

The experimental variogram of the dry biomass was computed using Equation 7 (Figure 6a). Several models were fitted to it by weighted least squares approximation using the program MLP (Ross, 1987), and the exponential model was found to provide the best fit in terms of Akaike's Information Criterion, AIC (Akaike, 1973) (Table 2). The nugget variance was removed from this model, and the spatially dependent component was regularized. The semivariance at a lag of one support is plotted against size of support in Figure 6a for 20 sizes of support. The maximum value of $\hat{\gamma}_v(v)$ is reached at approximately 11.5 m.

Many investigators measure the radiation over supports of around 0.5 m by 0.5 m (by measuring from a height of approximately 2 m with a 15° field-of-view (Milton, 1987)). The question is, Will this support capture the spatial variation of

interest? Is the spatial variation such that mapping with a support of 0.5 m by 0.5 m is futile? The spatial resolution at which $\hat{\gamma}_v(v)$ is maximized (11.5 m) indicates that the spatial resolution of 0.5 m by 0.5 m is appropriate in this instance: most of the spatially dependent variation will not be averaged within the support. The investigator can be confident that the spatial variation in the dry biomass will be captured if the support of the field radiometer measurements is 0.5 m by 0.5 m.

Consider a second scenario where the investigator wishes to map the dry biomass using airborne MSS imagery and the usual method based on regression (Curran and Williamson, 1987). As the flying height of the aircraft is variable, the investigator can choose a spatial resolution. Given the graph in Fig-
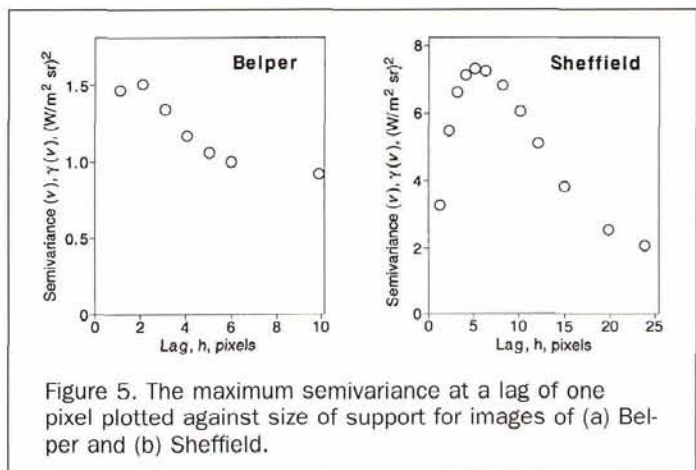

Figure 5. The maximum semivariance at a lag of one pixel plotted against size of support for images of (a) Belper and (b) Sheffield.
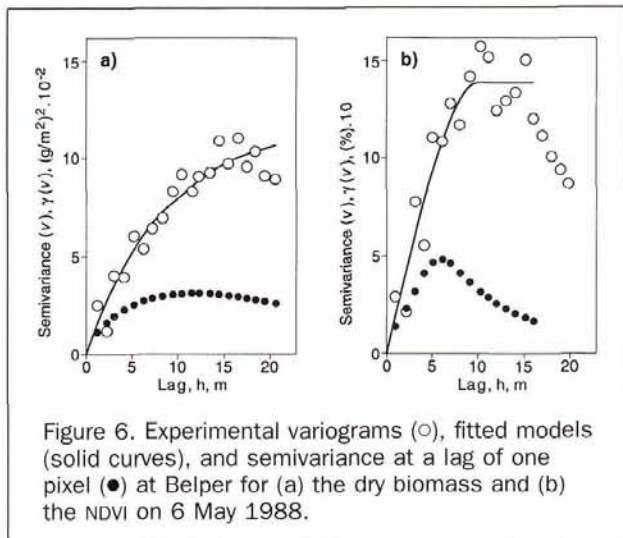
Figure 6. Experimental variograms (○), fitted models (solid curves), and semivariance at a lag of one pixel (●) at Belper for (a) the dry biomass and (b) the NDVI on 6 May 1988.

ure 6a, it is clear that, if the investigator wishes to capture the spatial variation in the dry biomass, the spatial resolution should be less than the lag at which $\hat{\gamma}_v(v)$ is maximized, probably 1 to 2 m. If this information were not available and a spatial resolution of 10 m was chosen, then most of the variation of interest would be lost and the investigation could be a waste of time and effort. If the aim is to use airborne MSS imagery and regression to map the percentage cover of clover, however, additional measurements must be made to compute the variogram. It is not available by default as for cokriging. If the cost of measuring the primary variable is too great, one might consider measuring instead the NDVI using field radiometry because the radiation must be correlated with the primary variable for remote sensing to be useful.

The experimental variogram of the NDVI is shown in Figure 6b. Several models were fitted to it, and the best fit was provided by the spherical model (Table 2). The spatially dependent component of this model was deregularized and regularized, and $\hat{\gamma}_v(v)$ was computed for several sizes of support and a graph was plotted (Figure 6b). The maximum is reached at a spatial resolution of 6 m, which is different from that for the dry biomass. The reason for this discrepancy is the difference in the shape of the two variograms. It may indicate that the NDVI is influenced by some property at the ground which has a component of spatial dependence with a shorter range of influence than that for the dry biomass, for example, moisture in the canopy. The example illustrates why the primary variable should be measured where possible.

On the basis of the above information, the investigator should choose a spatial resolution of much less than 6 m. For airborne sensor imagery such as that provided by the Daedelus AADS 1268 airborne MSS, this is likely to be the finest spatial resolution possible. If a spatial resolution of 10 m, for example, were chosen, most of the variation of interest would be encompassed within the support and, therefore, would not be detectable by analysis.

The examples presented above involve small area mapping. Most remote sensing for mapping is for large areas because the synoptic coverage provided is advantageous and

because most satellite sensors have a relatively coarse spatial resolution and a large area of coverage. The method presented can be applied to imagery recorded over larger areas, including choosing appropriate spatial resolutions for global remote sensing and even for new systems of sensing from satellite.

Conclusions

The variogram and $\hat{\gamma}_v(v)_{max}$ are proposed as aids to choosing appropriate spatial resolutions for mapping spatial variation by remote sensing. The advantages of modeling the spatial variation are as follows:

- Measurement error can be accounted for and treated separately from the underlying variation;
- The regularized variogram and $\hat{\gamma}_v(v)_{max}$ can be computed for any size of support, not just supports that are larger than and multiples of the original pixel size; and
- The regularized variogram and $\hat{\gamma}_v(v)_{max}$ can be computed for small sub-areas of images and for transect data.

In remote sensing investigations, it is desirable to determine an appropriate spatial resolution such that the information desired is acquired for least data. For mapping continuous variation by remote sensing, the support must be small enough to reveal the spatial variation of interest. The variogram and $\hat{\gamma}_v(v)_{max}$ can be used to define the predominant scale of spatial variation in a continuous variable, and to help ensure that the spatial resolution is chosen so that this scale of spatial variation is revealed in the data.

Acknowledgments

References

Akaike, H., 1973. Information theory and the extension of maximum liklihood principle, *Proceedings of the 2nd International Symposium on Information Theory* (B.N. Petrov and F. Csaki, editors), Akademia Kiado, Budapest, pp. 267–281.

Atkinson, P.M., 1993. The effect of spatial resolution on the experimental variogram of airborne MSS imagery, *International Journal of Remote Sensing*, 14:1005–1011.

———, 1995. A method for describing quantitatively the information, redundancy and error in digital spatial data, *Innovations in GIS II* (P. Fisher, editor), Taylor and Francis, London pp. 85–96.

Atkinson, P.M., and F.M. Danson, 1988. Spatial resolution for remote sensing of forest plantations, *Proceedings of the IGARSS '88 Symposium*, Edinburgh, Scotland, ESA Publications Division, Noordwijk, pp. 221–223.

Atkinson, P.M., P.J. Curran, and R.Webster, 1992. Cokriging with ground-based radiometry, *Remote Sensing of Environment*, 41:45–60.

Atkinson, P.M., and P.J. Curran, 1995. Defining an optimal size of support for remote sensing investigations, *IEEE Transactions on Geoscience and Remote Sensing*, 33:1–9.

Bizzell, R.M., and H.L. Prior, 1983. Thematic Mapper quality and performance assessment in renewable resources/agriculture/remote sensing, *Proceedings of the Landsat-4 Science Characterization Early Results Symposium*, Greenbelt, Maryland, NASA, 4:299–312.

Chavez, P.S., 1992. Comparison of spatial variability in visible and near-infrared spectral images, *Photogrammetric Engineering & Remote Sensing*, 58:957–964.

Clark, C.D., 1990. Remote sensing scales related to the frequency of natural variation: An example from paleo-ice-flow in Canada,

TABLE 2. MODELS FITTED TO EXPERIMENTAL VARIOGRAMS OF THE DRY BIOMASS AND NDVI AT BELPER ON 6 MAY 1988.

Variable	Model	c_0	c_1	a_1
dry biomass	Exponential	6.712	11.75	18.71
NDVI (6 May)	Spherical	14.59	13.87	10.01

IEEE Transactions on Geoscience and Remote Sensing, 28:503–515.

Clark, I., 1977. Regularization of a semi-variogram, *Computers and Geosciences,* 3:341–346.

Curran, P.J., 1988. The semi-variogram in remote sensing: an introduction, *Remote Sensing of Environment,* 37:493–507.

Curran, P.J., and H.D. Williamson, 1987. Airborne MSS data to estimate GLAI, *International Journal of Remote Sensing,* 8:57–74.

———, 1988. Selecting a spatial resolution for estimation of per-field green leaf area index, *International Journal of Remote Sensing,* 9:1243–1250.

Curran, P.J., and J.L. Dungan, 1989. Estimation of signal-to-noise: A new procedure applied to AVIRIS data, *IEEE Transactions on Geoscience and Remote Sensing,* 27:620–628.

Dungan, J.L., D.L. Peterson, and P.J. Curran, 1994. Alternative approaches for mapping vegetation quantities using ground and image data, *Environmental Information Management and Analysis: Ecosystem to Global Scales* (W. Michener, J. Brunt, and S. Stafford, editors), Taylor and Francis, London, pp. 237–261.

Gohin, F., and G. Langlois, 1993. Using geostatistics to merge in situ measurements and remotely-sensed observations of sea surface temperature, *International Journal of Remote Sensing,* 14:9–19.

Grieg-Smith, P., 1964. *Quantitative Plant Ecology,* Butterworths, London.

Gu, X.F., G. Guyot, and M. Verbrugghe, 1992. Evaluation of measurement errors in ground surface reflectance for satellite calibration, *International Journal of Remote Sensing,* 13:2531–2546.

Isaaks, E.H., and R.M. Srivastava, 1989. *Applied Geostatistics,* Oxford University Press, Oxford.

Johnson, D.D., and P.J. Howarth, 1987. The effects of spatial resolution on land cover/land use theme extraction from airborne digital data, *Canadian Journal of Remote Sensing,* 13:68–74.

Journel, A.G., and C.J. Huijbregts, 1978. *Mining Geostatistics,* Academic Press, London.

Jupp, D.L.B., A.H. Strahler, and C.E. Woodcock, 1988. Autocorrelation and regularization in digital images I. Basic theory, *IEEE Transactions on Geoscience and Remote Sensing,* 26:463–473.

———, 1989. Autocorrelation and regularization in digital images II. Simple image models, *IEEE Transactions on Geoscience and Remote Sensing,* 27:247–258.

Justice, C.O., B.L. Markham, J.R.G. Townshend, and R.L. Kennard, 1989. Spatial degradation of satellite data, *International Journal of Remote Sensing,* 9:1539–1561.

Lam, N.S.-N., and D.A. Quottrochi, 1992. On the issues of scale, resolution and fractal analysis in the mapping sciences, *Professional Geographer,* 44:88–98.

Latty, R.S., and R.M. Hoffer, 1981. Computer based classification accuracy due to the spatial resolution using per-point versus per-field classification techniques, *Machine Processing of Remotely Sensed Data Symposium,* West Lafayette, Indiana, pp. 384–393.

Matheron, G., 1965. *Les Variables Regionalisees et Leur Estimation,* Masson, Paris.

———, 1971. The theory of regionalized variables and its applications, *Cahiers du Centre de Morphologie Mathematique de Fontainebleau,* No. 5.

McGwire, K., M. Friedl, and J.E. Estes, 1993. Spatial structure, sampling design and scale in remotely sensed imagery of a Californian savanna woodland, *International Journal of Remote Sensing,* 14:2137–2164.

Mercer, W.B., and A.D. Hall, 1911. The experimental error of field trials, *Journal of Agricultural Science,* 4:107–132.

Milton, E.J., 1980. A portable multiband radiometer for ground data in remote sensing, *International Journal of Remote Sensing,* 1:153–165.

———, 1987. Principles of field spectroscopy, *International Journal of Remote Sensing,* 8:1807–1827.

Milton, E.J., and E.M. Rollin, 1987. *The Geophysical Environmental Reasearch Inc. IRIS Mk. IV Spectroradiometer: A Guide for UK Users,* University of Southampton, Southampton.

Moellering, H., and W.R. Tobler, 1972. Geographical variances, *Geographical Analysis,* 4:35–50.

Raffy, M., 1993. Remotely sensed quantification of covered areas and spatial resolution, *International Journal of Remote Sensing,* 14:135–159.

———, 1994. The role of spatial resolution in quantification problems: Spatialization method, *International Journal of Remote Sensing,* 15:2381–2392.

Ross, G.J.S., 1987. *Maximum Likelihood Program,* Numerical Algorithms Group, Oxford.

Rossi, R.E., D.J. Mulla, A.G. Journel, and E.H. Franz, 1992. Geostatistical tools for modeling and interpreting ecological spatial dependence, *Ecological Monographs,* 62:277–314.

Smith, H.F., 1938. An empirical law describing heterogeneity in the yields of agricultural crops, *Journal of Agricultural Science,* 28:1–23.

Strahler, A.H., C.E. Woodcock, and J.A. Smith, 1986. On the nature of models in remote sensing, *Remote Sensing of Environment,* 20:121–139.

Toll, D.L., 1983. Preliminary study of information extraction from Landsat TM data for a suburban/regional test site, *Proceedings of the Landsat-4 Science Characterization Early Results Symposium,* Greenbelt, Maryland, NASA 4:387–402.

Townshend, J.R.G., and C.O. Justice, 1988. Selecting the spatial resolution of satellite sensors required for global monitoring of land transformations, *International Journal of Remote Sensing,* 9:187–236.

Townshend, J.R.G., C.O. Justice, B.L. Markham, and S.A. Briggs, 1988. Spatial resolution requirements for MODIS-N, *Proceedings of the 4th International Colloquium on Spectral Signatures of Objects in Remote Sensing,* ESA, Aussois, France, Noordwijk, pp. 329–331.

Vogt, J., 1992. *Characterizing the Spatio-Temporal Variability of Surface Parameters from NOAA AVHRR Data,* Joint Research Center, Ispra, Italy.

Von Neuman, J., 1941. Distribution of the ratio of the mean square successive difference, *Annals of Mathematical Statistics,* 12:367–395.

Webster, R., 1991. Local disjunctive kriging of soil properties with change of support, *Journal of Soil Science,* 42:301–318.

Webster, R., P.J. Curran, and J.W. Munden, 1989. Spatial correlation in reflected radiation from the ground and its implications for sampling and mapping by ground-based radiometry, *Remote Sensing of Environment,* 29:67–78.

Webster, R., and M.A. Oliver, 1990. *Statistical Methods for Soil and Land Resources Survey,* Oxford University Press, Oxford.

Welch, R., 1982. Spatial resolution requirements for urban studies, *International Journal of Remote Sensing,* 3:139–146.

Woodcock, C.E., and A.H. Strahler, 1987. The factor of scale in remote sensing, *Remote Sensing of Environment,* 21:311–322.

Zhang, R., A.W. Warrick, and D.E. Myers, 1990. Variance as a function of sample support size, *Mathematical Geology,* 22:107–122.